

Competition-induced shifts of spectral peaks in photon coincidence spectroscopy

Levente Horvath and Barry C. Sanders

Department of Physics, Macquarie University, Sydney, New South Wales 2109, Australia

(Dated: Received: 2000 / Revised version:)

We show that shifts in locations of two-photon coincidence spectral peaks, for a bichromatically-driven two-level atom passing through a single-mode cavity, are due to competition between excitation pathways for a Jaynes-Cummings system. We also discuss an analogous shift of (single-photon) spectral peaks for a driven three-level V -system, which demonstrates that competition between excitation pathways is also important in this simple system.

PACS numbers: 42.50.Ct, 42.50.Dv

I. INTRODUCTION

Cavity quantum electrodynamics (CQED) has continued to develop rapidly, driven both by recent experimental successes and by the promise of exciting new applications. Advances in atom cooling techniques, as well as development of high-Q optical cavities with large-dipole coupling, have enabled testing of the strong-coupling regime of CQED [1] as well as the trapping of single atoms in optical cavities [2, 3].

Applications of CQED, especially for such applications as the quantum logic gate [4], rely critically on entanglement between the field degree of freedom and the internal electronic state of the atom [5, 6]. This entanglement is not only challenging to achieve, it is also difficult to probe. In the optical regime of CQED, photon coincidence spectroscopy (PCS) has been proposed as a feasible and unambiguous method for detecting genuine quantum phenomena in CQED. This technique employs a bichromatic (or multichromatic) driving field acting on the combined atom-cavity system and detects two-photon (or multiphoton) decays, respectively, by registering photon coincidences in the cavity field emission [6, 7, 8].

The simplest case of PCS is two-photon coincidence spectroscopy (2PCS) for probing the nonlinear portion of the Jaynes-Cummings (JC) spectrum. The technique of 2PCS proceeds, first by driving the atomic beam with a bichromatic field (consisting of a fixed driving field with fixed frequency ω_1 and a scanning field with tunable frequency ω_2), which causes two-photon excitation to the second couplet of the JC ladder, followed by two-photon decay from the atom-cavity system (Fig. 1). The objective is to count photon pairs emitted from the cavity as a function of varying ω_2 . When the sum frequency for the bichromatic driving field $\omega_1 + \omega_2$ matches a transition frequency from the second couplet in the JC spectrum to the ground state, the result is an enhanced two-photon count rate (2PCR).

This simple picture of excitation pathways agrees with simulations [6, 7], but displacement of coincidence peaks as a function of scanning field frequency was evident yet not properly understood [6]. Here we show that the deviation of peak shifts is due to competition between excitation pathways. This picture yields excellent quantitative

agreement with simulations of 2PCS.

II. MASTER EQUATION AND TWO-PHOTON COUNT RATES

In the electric-dipole and rotating-wave approximations, the JC Hamiltonian for the two-level atom (2LA) coupled with the single mode is

$$H(g) = \omega(\sigma_z + a^\dagger a) + ig(\mathbf{r})(a^\dagger \sigma_- - a \sigma_+), \quad (1)$$

with \mathbf{r} the position of the atom, $g(\mathbf{r})$ the position-dependent dipole coupling strength, a and a^\dagger the annihilation and creation operators for photons in the cavity field, σ_+ , σ_- , and σ_z the 2LA raising, lowering and inversion operators, respectively, and $\hbar = 1$. Provided that the atoms move sufficiently slowly through the cavity [6, 7], the atom can be treated as if it were at rest at some randomly located position \mathbf{r} . As the position \mathbf{r} is a randomly varying quantity, the value of the coupling strength g itself is also random. Hence, a coupling strength distribution $P(g)$ can be constructed [7], and we assume the $P(g)$ depicted in Fig. 5 of Ref. [7]. This $P(g)$ corresponds to the coupling strength distribution obtained for atoms passing through a rectangular mask, centered at an antinode, for the cavity sustaining only the TEM₀₀ mode. The dimension of the mask is w_0 (cavity mode waist) by $\lambda/10$ (with λ the optical wavelength). We restrict $Fg_{\max} < g < g_{\max}$ for g_{\max} the coupling strength at an antinode along the cavity longitudinal axis and F an effective cut-off term.

The spectrum for the Hamiltonian (1), depicted in Fig. 1, is the well-known JC spectrum, or ‘ladder’ [9]. The ‘dressed states’ of the combined atom-cavity system are here designated by the lowest-energy state $|0\rangle \equiv |0\rangle_{\text{cav}} \otimes |g\rangle_{\text{atom}} \equiv |0, g\rangle$, and, for n a positive integer, the ‘excited’ states $|n\rangle_{\pm} \equiv i/\sqrt{2} (|n-1, e\rangle \pm i |n, g\rangle)$, with $|n\rangle$ the Fock state of the cavity mode and $|g\rangle$ ($|e\rangle$) the ground (excited) state of the 2LA. The effect of averaging over $P(g)$ is an inhomogeneous spectral broadening, due to atomic position variability, as shown in Fig. 1.

Two-photon excitation is provided by driving the atom directly, as it traverses the cavity, with a bichromatic field $\mathcal{E}(t) = \mathcal{E}_1 e^{-i\omega_1 t} + \mathcal{E}_2 e^{-i\omega_2 t}$. The driving-field frequency ω_1 is fixed and resonantly excites the atom-cavity

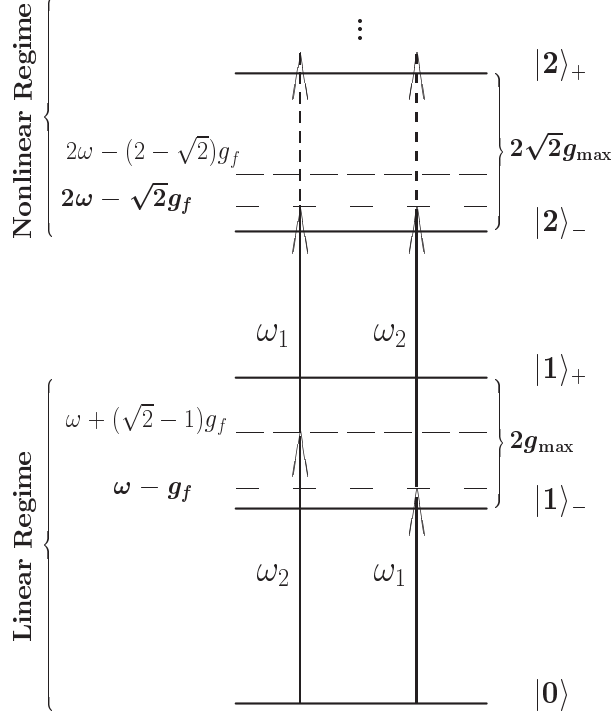


FIG. 1: Two-photon excitation scheme from the ground state $|0\rangle$ to the first two excited couplets $|n\rangle_\varepsilon$ ($n \in \{1, 2\}$, $\varepsilon \in \{-, +\}$) of the dressed states. The inhomogeneous broadening of the couplets $|1\rangle_\varepsilon$ and $|2\rangle_\varepsilon$ is $2\hbar g_{\max}$ and $2\sqrt{2}\hbar g_{\max}$, respectively. Two two-photon excitations to the second couplet are depicted for a bichromatic driving field with one component of amplitude \mathcal{E}_1 and the other with amplitude \mathcal{E}_2 . The excitation pathway on the right (ω_1 then ω_2) excites resonantly from $|0\rangle$ to $|1\rangle_-$ and then may excite resonantly to either $|2\rangle_\pm$. The excitation pathway on the left (ω_2 then ω_1) excites resonantly from $|0\rangle$ to $|1\rangle_+$ to $|2\rangle_-$ for $g = (\sqrt{2}-1)g_f$.

system from the ground state $|0\rangle$ to the excited state $|1\rangle_-$ for the subensemble $g = g_f = \omega - \omega_1$; this subensemble corresponds to $P(g) = \delta(g - g_f)$.

The scanning-field frequency is ω_2 , and excites the subensemble for $g = g_f$ from $|1\rangle_-$ to one of the two states in the second couplet of the JC ladder, namely $|2\rangle_\pm$. Thus, the range of scanning frequencies for ω_2 must include the $|1\rangle_- \leftrightarrow |2\rangle_\pm$ transition frequencies, $\omega \pm (\sqrt{2} \mp 1)g$, respectively. The amplitudes of the two chromatic components should be large enough to ensure sufficient occupation of the excited state but not large enough that significant Stark shifting or nonnegligible occupation of the higher-order states occurs. Enhanced rates of photon pair detection are then sought as the scanning frequency ω_2 is varied such that $\omega_1 + \omega_2$ is resonant with some transition $|0\rangle \leftrightarrow |2\rangle_\pm$ as depicted in Fig. 1.

The Born-Markov approximation is applied to both radiation reservoirs: the reservoir for the field leaving the

cavity and the reservoir for direct fluorescence of the 2LA from the sides of the cavity into free space. The cavity damping rate is κ , and the cavity-inhibited spontaneous emission rate into free space is γ . The master equation for this system [7] can be expressed as $\dot{\rho} = \mathcal{L}\rho$ for \mathcal{L} the Liouville operator. Here $\mathcal{L} = \mathcal{L}_{\text{eff}} + \mathcal{D} + \mathcal{J}$, i.e. a sum of a Liouville operator \mathcal{L}_{eff} , an explicit time-dependent Liouville operator \mathcal{D} and a ‘jump’ term \mathcal{J} . We introduce $\delta \equiv \omega_2 - \omega_1$ and work in the rotating picture with respect to the driving-field component ω_1 .

The effective Hamiltonian is (without jump terms)

$$H_{\text{eff}}(g, \mathcal{E}_1) = (\omega - \omega_1)(\sigma_z + a^\dagger a) + \Xi(g) + \Upsilon(\mathcal{E}_1) - i\kappa a^\dagger a - i(\gamma/2)\sigma_+\sigma_-, \quad (2)$$

for $\Xi(g) = ig(a^\dagger\sigma_- - a\sigma_+)$ the quantum exchange operator and $\Upsilon(\mathcal{E}_1) = i\mathcal{E}_1(\sigma_+ - \sigma_-)$ a monochromatic 2LA driving term. The corresponding Liouville operator is

$$\mathcal{L}_{\text{eff}}(g, \mathcal{E}_1)\rho = -i[H_{\text{eff}}(g, \mathcal{E}_1)\rho - \rho H_{\text{eff}}^\dagger(g, \mathcal{E}_1)]. \quad (3)$$

The operator for the jump term is \mathcal{J} such that

$$\mathcal{J}\rho = 2\kappa a\rho a^\dagger + \gamma\sigma_-\rho\sigma_+, \quad (4)$$

and the time-dependent Liouville operator is $\mathcal{D}(t)$ such that

$$\mathcal{D}\rho = -i[\Upsilon(\mathcal{E}_2 e^{-i\delta t}), \rho]. \quad (5)$$

Solving the master equation for $\dot{\rho}$, and averaging over $P(g)$, which accounts for atomic position variability, yields a solution

$$\bar{\rho} \equiv \int_{Fg_{\max}}^{g_{\max}} P(g)\rho(g)dg. \quad (6)$$

For a bichromatic driving field, the density matrix does not settle to a steady state value, but in the long-time limit $t \rightarrow \infty$, the Bloch function expansion is

$$\lim_{t \rightarrow \infty} \bar{\rho}(t) = \sum_{m=-\infty}^{\infty} \bar{\rho}_m e^{im\delta t}, \quad (7)$$

with $\bar{\rho}_m$ time-independent matrices. As the photocount integration time is expected to be long compared to the detuning δ , it is reasonable to assume that rapidly oscillating terms average out and therefore approximate $\rho(g)$ by truncating the expansion (7).

The optical signature for entanglement is the 2PCR [8],

$$w^{(2)}(\delta, \mathcal{E}_1) = \langle : n^2 : \rangle(\delta, \mathcal{E}_1), \quad (8)$$

for $n \equiv a^\dagger a$. The 2PCR is shown in Fig. 2 as a dotted line, and the peaks expected at $\tilde{\delta} = (\delta - g_f)/g_f = \pm(\sqrt{2} - 1)$ are not distinguishable. This indistinguishability is due to off-resonant two-photon transitions with both photons of frequency ω_2 , and may be overcome via the

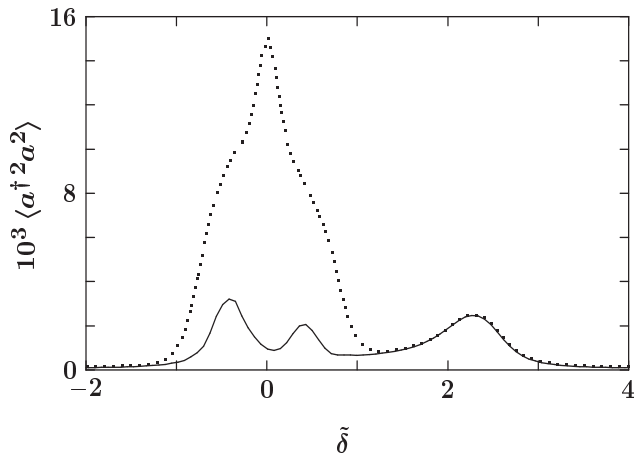


FIG. 2: The 2PCR vs the normalized detuning $\tilde{\delta}$ for the inhomogeneously broadened system, with $\mathcal{E}_1/\kappa = 1/\sqrt{2}$, $\mathcal{E}_2/\kappa = \sqrt{2}$, $g_f/\kappa = 9$, $\gamma/\kappa = 2$: $w^{(2)}(\delta, \mathcal{E}_1)$ is the solid line and $\Delta^{(2)}(\delta, \mathcal{E}_1)$ is the dotted line.

method of background subtraction: the experiment is repeated with $\mathcal{E}_1 = 0$ and the resultant 2PCR subtracted. Thus, we define a difference-2PCR

$$\Delta^{(2)}(\delta, \mathcal{E}_1) = w^{(2)}(\delta, \mathcal{E}_1) - w^{(2)}(\delta, \mathcal{E}_1 = 0). \quad (9)$$

For a specific set of parameters we show in Fig. 2 the 2PCR with and without background subtraction, which is significant in the domain of homogeneous broadening $-1 \leq \tilde{\delta} \leq 1$, but the region near $\tilde{\delta} = 1 + \sqrt{2}$ is not significantly affected by background subtraction. Background subtraction helps to resolve the two two-photon spectral peaks at $\tilde{\delta} = \pm(\sqrt{2} - 1)$.

III. COMPETITION-INDUCED SPECTRAL PEAK SHIFTS

The objective of 2PCS is to obtain a 2PCR with peaks at values of $\tilde{\delta}$ which cannot be explained by semiclassical models. The peaks at $\tilde{\delta} = \pm(\sqrt{2} - 1)$ and $\tilde{\delta} = \sqrt{2} + 1$ involve the quantity $\sqrt{2}$, which follows from the quantum field expression $a|2\rangle = \sqrt{2}|1\rangle$. This $\sqrt{2}$ is therefore a genuine, unambiguous quantum field signature. However, the actual peaks in 2PCR cannot be expected to occur at exactly these values of $\tilde{\delta}$ as observed quite clearly in Fig. 5 of Ref. [6]. In Fig. 3 we show in detail the peak near $\tilde{\delta} = \sqrt{2} + 1$ as a solid line for $P(g) = \delta(g - g_f)$ and an anomalous shift from its expected position at $\tilde{\delta} = \sqrt{2} + 1$, or $\Delta\tilde{\delta} \equiv \tilde{\delta} - (\sqrt{2} + 1) = 0$, is evident. We begin exploring this anomalous shift for the $g = g_f$ subensemble.

We observe that this peak is noticeably shifted from the expected location. The origin of the shifts in peaks is subtle. In Ref. [6] the suggestion is that “the peaks are shifted slightly, probably due to the motion of atoms”.

Although atomic motion may contribute to peak shifts, we show in this section that competition between excitation pathways is the major factor in shifts of 2PCS peaks.

The peak at $\tilde{\delta} = \sqrt{2} + 1$ is the most interesting of the three major 2PCR peaks (i) because background subtraction is not required to detect this peak (as $\tilde{\delta}$ lies outside the region of inhomogeneous broadening) and (ii) because the peak is quite distinct from the large neighboring pair of peaks at $\tilde{\delta} = \pm(\sqrt{2} - 1)$. The excitation pathway to obtain the peak at $\tilde{\delta} = \sqrt{2} + 1$ is via an ω_1 photon which resonantly excites $|0\rangle \leftrightarrow |1\rangle_-$, followed by an ω_2 photon which resonantly excites $|1\rangle_- \leftrightarrow |2\rangle_+$ for the 2PCR peak at $\tilde{\delta} = \sqrt{2} + 1$ as shown in Fig. 1. However, level $|2\rangle_-$ becomes populated as well as $|2\rangle_+$ by off-resonant excitation.

The competition between populating levels $|2\rangle_{\pm}$ is evident in Figs. 3(d,e) of Ref. [7], which depict the populations of levels $|2\rangle_{\pm}$ as functions of g and $\tilde{\delta}$. The $|2\rangle_-$ level is noticeably occupied for all values of $\tilde{\delta}$ for g in the vicinity of g_f . This occupation of $|2\rangle_-$ was not explicitly discussed in Ref. [6, 7], and the significance of this population of $|2\rangle_-$ was not provided with respect to the shift in the peak at $\tilde{\delta} = \sqrt{2} + 1$. The shift in the peak is shown but not discussed in Ref. [7]. The following analysis provides the first detailed picture for explaining the shift in the 2PCR peaks.

The effect of competition is made clear in Fig. 3. Here we present one portion of the 2PCR peak as a function of $\tilde{\delta}$, in the vicinity of $\Delta\tilde{\delta} = 0$. The solid line corresponds to the 2PCS. The dotted line corresponds to the simulated 2PCS but with the artificial restriction that the matrix elements of the Hamiltonian driving field operator $\Upsilon(\mathcal{E}_2 \exp(-i\delta t))$ for the transition $|1\rangle_- \leftrightarrow |2\rangle_-$ are set to zero. That is, we artificially impose the condition

$$-\langle 1|\Upsilon(\mathcal{E}_2 \exp(-i\delta t))|2\rangle_- = 0 = -\langle 2|\Upsilon(\mathcal{E}_2 \exp(-i\delta t))|1\rangle_- . \quad (10)$$

By doing so we observe, and show in Fig. 3, that the modified 2PCS graph is indeed centered at $\Delta\tilde{\delta} = 0$ (equivalently, at $\tilde{\delta} = \sqrt{2} + 1$). The comparison between the two cases, with both $-\langle 1|\Upsilon(\mathcal{E}_2 \exp(-i\delta t))|2\rangle_-$ and its conjugate set to zero vs both not being set to zero, provides convincing evidence that the shift in the peak is indeed primarily due to competition between two excitation pathways.

Thus far our attention has been restricted to the $P(g) = \delta(g - g_f)$ case. This case is a significant contributor to the peak shift for the inhomogeneously-broadened peak shift obtained in the full simulation, accounting for atomic position variability. The simulation of the 2PCR peak near $\tilde{\delta} = \sqrt{2} + 1$ is depicted in Fig. 4(a) as a solid line. This solid line evidently has a peak at $\Delta\tilde{\delta} = -0.141$. The above reasoning, for the $P(g) = \delta(g - g_f)$ case, suggests that the competing pathway $|1\rangle_- \leftrightarrow |2\rangle_-$ is partially responsible for this peak shift. Therefore, we repeat the simulation, but with the restriction (10). The result of this simulation is also depicted in Fig. 4(a) as

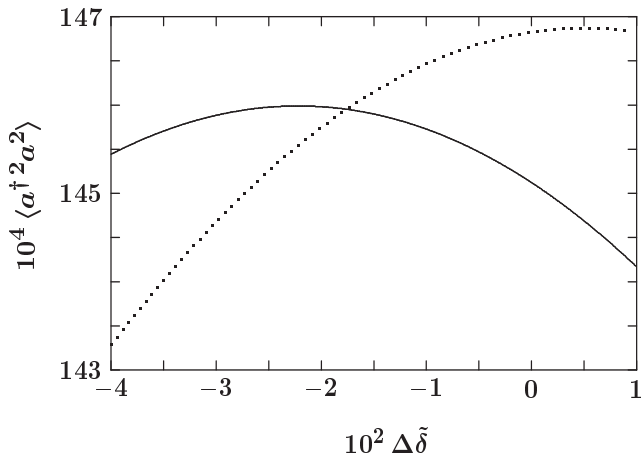


FIG. 3: Two-photon count rate (2PCR) vs the shift in normalized scanning frequency of the peak at $\tilde{\delta} = \sqrt{2} + 1$ for $g/\kappa = 9$, $\mathcal{E}_1/\kappa = 1/\sqrt{2}$, $\mathcal{E}_2/\kappa = \sqrt{2}$ and $\gamma/\kappa = 2$ depicted as the solid line. The dotted line corresponds to the case with condition (10) imposed.

a dashed line. The new peak position is located approximately at $\Delta\tilde{\delta} = -0.094$. This peak position can be shifted slightly by eliminating other pathways. By fixing all transition terms of the type (10) to be zero *except* for $\langle 0|\Upsilon(\mathcal{E}_1)|1\rangle_-$, $-\langle 1|\Upsilon(\mathcal{E}_2 \exp(-i\delta t))|2\rangle_+$, and their complex conjugates, the resultant peak is centered at $\Delta\tilde{\delta} = -0.091$. These additional pathways, which were ignored in obtaining $\Delta\tilde{\delta} = -0.094$, do not contribute much to the overall peak shift, and we do not depict this specific peak shift.

To account for the remainder of the peak shift observed in Fig. 4(a), we determine other pathways to an enhanced 2PCR, which arise in the full inhomogeneously broadened case but not in the $g = g_f$ case. We now consider the effect of the homogeneous linewidth at the level $|1\rangle_-$ state. To incorporate this effect, we solve the dynamics for the effective Hamiltonian (2) plus the driving term (5) but do not include the jump term (4). The 2PCR, which eliminates the pathway $|1\rangle_- \longleftrightarrow |2\rangle_-$ and the homogeneous linewidth at $|1\rangle_-$ is depicted in Fig. 4(b). We observe that the resultant peak shift is now $\Delta\tilde{\delta} = -0.057$. The consideration of the homogeneous linewidth does matter in accounting for the peak shift.

To understand the peak shift due to the homogeneous linewidth at $|1\rangle_-$, we consider the following. The pathway $|0\rangle \longleftrightarrow |1\rangle_- \longleftrightarrow |2\rangle_+$ is relatively unaffected by the homogeneous linewidth as it is a resonant transition at $\Delta\tilde{\delta} = 0$, but the homogeneous linewidth does enable off-resonant excitation to $|2\rangle_-$, even after the restriction (10) has been applied. The homogeneous linewidth of the $|1\rangle_-$ level enables two-photon transitions to take place for a range of coupling strength g , via the sequence of an ω_1 photon and then an ω_2 photon. By eliminating this homogeneous linewidth, the ω_1 photons really must satisfy the condition $\omega - \omega_1 = g_f$ in order to off-

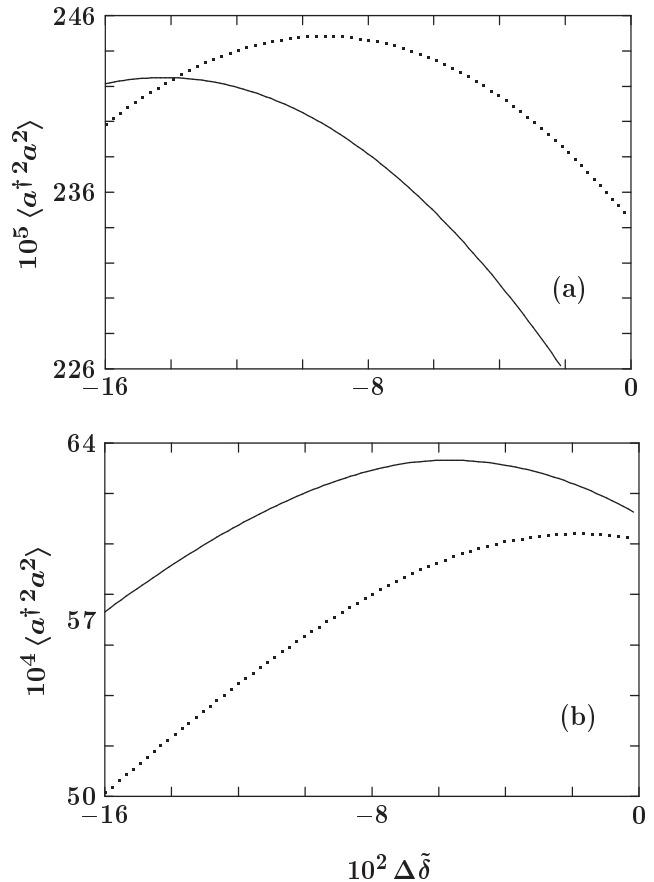


FIG. 4: The 2PCR vs peak shift from $\tilde{\delta} = \sqrt{2} + 1$ for the inhomogeneously broadened system with $\mathcal{E}_1/\kappa = 1/\sqrt{2}$, $\mathcal{E}_2/\kappa = \sqrt{2}$, $g_f/\kappa = 9$, $\gamma/\kappa = 2$. Two cases are shown: (a) with (solid) and without (dots) the imposition of condition (10); and (b) with the imposition of condition (10) and the homogeneous linewidth (and jump terms) set to zero for the $|1\rangle_-$ level of the JC ladder (solid), and with the additional imposition that $\langle 0|\Upsilon(\mathcal{E}_2 \exp(-i\delta t))|1\rangle_+$ and its complex conjugate are set to zero (dots).

resonantly excite to the $|2\rangle_-$ level. The homogeneous linewidth is responsible for permitting competing pathways from $|0\rangle \longleftrightarrow |1\rangle_- \longleftrightarrow |2\rangle_-$ for a range of g values, and eliminating this homogeneous linewidth eliminates a whole class of competing pathways for the inhomogeneously broadened (general $P(g)$) system.

The final significant contribution to the peak shift of the 2PCR curve arises for small g . The low coupling strength limit is important because the distribution $P(g)$ is so heavily weighted in favor of low g . When the coupling strength is small, the splitting between the first couplet states $|1\rangle_{\pm}$ becomes correspondingly small. Consequently one would expect a competing pathway to arise via excitation to $|1\rangle_+$. We eliminate the contribution due to the pathway $|0\rangle \longleftrightarrow |1\rangle_+$. Incorporating this restriction with the other restrictions previously mentioned (eliminating the $|1\rangle_- \longleftrightarrow |2\rangle_-$ pathway and the homogeneous linewidth at $|1\rangle_-$) leads to the dotted curve in Fig. 4(b). The resultant peak shift is just $\Delta\tilde{\delta} = -0.018$.

The three effects considered above account for 87% of the peak shift. Better agreement can be obtained by reducing homogeneous linewidth on the $|2\rangle_-$ level or by eliminating transitions to the competing state $|2\rangle_-$ altogether. However, the agreement demonstrated here exhibits excellent agreement with the full simulated 2PCR peak at $\tilde{\delta} = \sqrt{2} + 1$. There is no doubt that this shift is primarily due to competing pathways in the JC ladder.

In accounting for the peak shift due to competing pathways, we have included restrictions of coherent transitions and thereby accounted for the majority of the peak shift. There is also competition with incoherent pathways, which are accounted for by the quantum jump terms. The quantum jumps correspond to the transfer of quanta between levels of the JC ladder, but the contribution of these jumps to peak shifts is not large for the bichromatically-driven JC system. Never the less, the jump terms are responsible for part of the peak shift. This competition with incoherent pathways is quite pronounced for the monochromatically-driven three-level system discussed in the next section.

IV. THE MONOCHROMATICALLY-DRIVEN THREE-LEVEL V -SYSTEM

The shift in spectral peaks should not be unique to a bichromatically-driven JC system. A simple case to consider is the monochromatically-driven three-level V -system (the JC ladder in the linear regime, cf Fig. 1), which is of interest for studying normal-mode (or vacuum Rabi) splitting [10, 11, 12].

We consider the three-level truncation of the JC ladder to $\{|0\rangle, |1\rangle_{\pm}\}$ and a monochromatic driving field which is resonant with the $|0\rangle \longleftrightarrow |1\rangle_+$ transition ($\omega_1 = \omega + g_f$) where ω_1 is allowed to vary. In contrast to the previous section, enhanced one-photon count rates identify resonances and correspond to the standard method of spectroscopy, as opposed to photon *coincidence* spec-

troscopy. The normalized frequency of this driving field is $\tilde{\delta} = -\delta/g_f$ for $\delta = \omega - \omega_1$. We expect a peak at $\tilde{\delta} = 1$, for which resonant excitation occurs if we ignore competition between excitation pathways.

In Fig. 5 we see that, for $\Delta\tilde{\delta} = \tilde{\delta} - 1$, the peak is shifted to the left. Competition due to off-resonant excitation is established by setting certain matrix elements of the driving term in the master equation to zero, by analogy with the 2PCR considered above. That is, for $H_{\text{eff}}(g, \mathcal{E}_1)$ in Eq. (2), we impose

$$\langle 0|\Upsilon(\mathcal{E}_1 \exp(-i\delta t))|1\rangle_- = 0 = -\langle 1|\Upsilon(\mathcal{E}_1 \exp(-i\delta t))|0\rangle \quad (11)$$

in the simulation. We observe that this condition produces a plot of $\langle a^\dagger a \rangle$ that is exactly centered at $\Delta\tilde{\delta} = 0$. Therefore, the competition with the off-resonant excitation pathway $|0\rangle \longleftrightarrow |1\rangle_-$ is entirely responsible for the peak shift of $\langle a^\dagger a \rangle$ vs $\tilde{\delta}$.

Another perspective for understanding the spectral peak shift for the driven V -system is obtained directly from the effective Hamiltonian of Eq. (2) solved in the linear regime. We define for the pseudo-pure state ψ , $C_0 \equiv \langle 0|\psi\rangle$ and $C_{1\pm} \equiv \langle 1|\psi\rangle$. The resulting set of differential equations for these dressed-state amplitudes C_0 , C_{1-} and C_{1+} is given by

$$\dot{C}_0 = -\frac{\mathcal{E}_1}{\sqrt{2}}(C_{1-} + C_{1+}), \quad (12)$$

$$\begin{aligned} \dot{C}_{1-} &= \frac{\mathcal{E}_1}{\sqrt{2}}C_0 - \left(i(\delta - g) + \frac{1}{2} \left(\kappa + \frac{\gamma}{2} \right) \right) C_{1-} \\ &\quad + \frac{1}{2} \left(\kappa - \frac{\gamma}{2} \right) C_{1+} \end{aligned} \quad (13)$$

$$\begin{aligned} \dot{C}_{1+} &= \frac{\mathcal{E}_1}{\sqrt{2}}C_0 - \left(i(\delta + g) + \frac{1}{2} \left(\kappa + \frac{\gamma}{2} \right) \right) C_{1+} \\ &\quad + \frac{1}{2} \left(\kappa - \frac{\gamma}{2} \right) C_{1-}. \end{aligned} \quad (14)$$

Taking the Laplace transform in the long time limit, a minimum and two maxima occur in the PCR for

$$\tilde{\delta} = \tilde{\delta}_0 \equiv 0 \text{ (minimum)}, \quad (15)$$

$$\tilde{\delta} = \tilde{\delta}_{\pm} \equiv -\sqrt{1 \pm \frac{2 + \mathcal{E}^2}{2g^2}} \text{ (maxima)}, \quad (16)$$

for the decay rate $\gamma/\kappa = 2$. To identify competition between pathways, we impose the condition Eq. (11). This condition modifies Eq. (12) by replacing the C_{1-} term by zero and modifies Eq. (13) by replacing C_0 by zero. The peak at $\tilde{\delta}_-$ thus vanishes, as there is no driving to the $|1\rangle_-$ state. The peak at $\tilde{\delta}_+$ is shifted to $\tilde{\delta} = 1$ (where the peak would be expected initially without any competition between excitation pathways). The formula for the competition-induced peak shift for the three-level JC system is thus given by

$$\Delta\tilde{\delta} = \tilde{\delta}_+ - 1 = \sqrt{1 - \frac{2 + \mathcal{E}^2}{2g^2}} - 1. \quad (17)$$

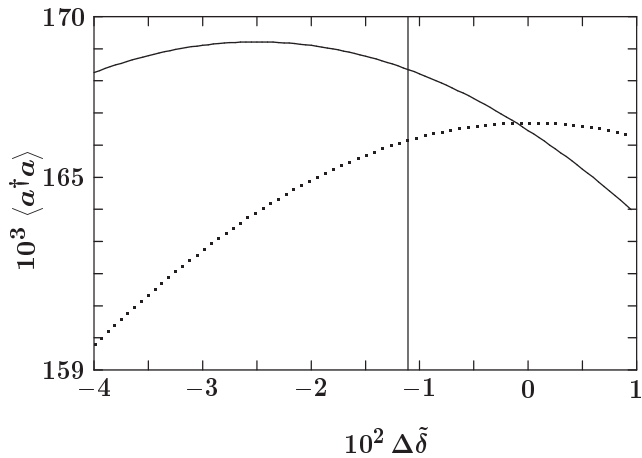


FIG. 5: One-photon count rate (IPCR) of a three-level system vs the shift in normalized scanning frequency of the peak at $\tilde{\delta} = 1$ for $g/\kappa = 9$, $\mathcal{E}_1/\kappa = \sqrt{2}$ and $\gamma/\kappa = 2$ depicted as the solid line. The dotted line corresponds to the case $\langle 0|\Upsilon(\mathcal{E}_1 \exp(-i\delta t))|1\rangle_- = 0 = \langle 1|\Upsilon(\mathcal{E}_1 \exp(-i\delta t))|0\rangle$. The vertical line corresponds to $\Delta\tilde{\delta}$ in Eq. (17).

The peak shift $\Delta\tilde{\delta}$ presented in Eq. (17) accounts partially for the total peak shift presented in Fig. (5). The discrepancy is due solely to the effect of quantum jump terms, which have been ignored in Eqs. (15)–(16). The necessity of including quantum jump terms arises because dissipation terms cannot be dissociated from fluctuations in a proper analysis. The quantum jump terms are responsible for incoherent transitions of quanta from one level to another of the three-level system. We observe, in Eqs. (15)–(16), that incoherent transitions are not included in the mathematics. Specifically, we can see that diagonal matrix elements $\rho_{00} = C_0^* C_0$ and $\rho_{11}^{\pm\pm} = C_{1\pm}^* C_{1\pm}$ are not coupled together. This coupling of diagonal elements of the density matrix arises via quantum jump terms. These quantum jump terms are responsible for the discrepancy between the predicted peak shift given by Eq. (17) and the observed peak center of the solid locus in Fig. 5. Whereas, for the bichromatically-driven JC system, the contribution of incoherent pathways to the net peak shift is small, the contribution of incoherent pathways to the peak shift for the monochromatically-driven three-level \vee system is relatively large because there are fewer coherent pathways to producing a peak shift as compared to the bichromatically-driven JC system considered in the previous section.

The advantage of using Eqs. (15)–(16), to confirm that the peak shift is indeed partially due to competition between coherent excitation pathways, is that this method is entirely analytical. The analytical method provides a simpler conceptual framework to understand the role of both coherent and incoherent excitation pathways. In this analytical method, we obtain solutions via the Laplace transform method rather than relying on nu-

merical solutions to the full master equation. Numerical methods are necessary, though, to fully account for spectral peak shifts.

V. CONCLUSION

The analysis presented here provides convincing evidence that the shifts in two-photon coincidence spectral peaks, from expected locations suggested by the JC ladder of Fig. 1, are due overwhelmingly to competition between excitation pathways.

We have analyzed in detail the two-photon spectral peaks, outside the domain where background subtraction is essential for resolution. The shift of the spectral peak has been shown to be a consequence of competition between excitation pathways. This demonstration relies on numerical methods whereby the competing pathway have been artificially eliminated by imposing the condition that certain matrix elements are zero in the master equation.

The key contribution to the peak shift were identified to be competition with the $|0\rangle \longleftrightarrow |1\rangle_- \longleftrightarrow |2\rangle_-$ pathway for $g \approx g_f$, $|0\rangle \longleftrightarrow |1\rangle_+ \longleftrightarrow |2\rangle_{\pm}$ for $g \rightarrow 0$ and the homogeneous linewidth about $|1\rangle_-$ which allowed off-resonant excitation to $|2\rangle_{\pm}$. Eliminating these three effects reduces the two-photon coincidence peak shift by 87%.

These shifts in spectral peaks are not restricted to 2PCS. To verify this, we considered the shifts of spectral peaks for standard (one-photon) spectroscopy and a three-level monochromatically-driven \vee -system. Such a system corresponds to the driven JC system in the linear regime, which is of interest in the study of normal-mode (vacuum Rabi splitting). We also observe the shift of spectral peaks in our simulations. By ignoring the jump terms, the equations become easily solvable and we verify that a significant part of the peak shift for the \vee -system are indeed due to competition between excitation pathways. The analytical method enables us to clearly see the distinction between coherent and incoherent pathways as competition-induced peak shifts. The contribution of quantum jump terms to the net peak shift is significant for the monochromatically-driven \vee system, whereas the effect is much smaller for the bichromatically-driven JC system. The combination of competition with coherent and incoherent pathways fully accounts for the peak shift of the monochromatically-driven three-level \vee system analyzed in Sec. IV.

These results clarify the expected peak locations in 2PCS and should also apply to the more general Multiphoton Coincidence Spectroscopy [8]. As photon coincidence spectroscopy must be accurate to verify the signature of entanglement, these peak shifts must be fully accounted for and properly understood. The analysis presented here does indeed explain the peak shifts clearly and quantitatively.

Acknowledgments

We acknowledge useful discussions with H. J. Carmichael, Z. Ficek, K.-P. Marzlin and Weiping Zhang.

This research has been supported by Australian Research Council Large and Small Grants and by an Australian Research Council International Research Exchange Scheme Grant.

-
- [1] R. J. Thompson, Q. A. Turchette, O. Carnal, and H. J. Kimble, *Phys. Rev. A*, **57**, 3084 (1998).
 - [2] C. J. Hood, T. W. Lynn, A. C. Doherty, A. S. Parkins, and H. J. Kimble, *Science* **287**, 1447 (2000).
 - [3] P. W. H. Pinkse, T. Fischer, P. Maunz, and G. Rempe, *Nature* **404**, 365 (2000).
 - [4] Q. A. Turchette, C. J. Hood, W. Lange, H. Mabuchi, and H. J. Kimble, *Phys. Rev. Lett.* **75**, 4710 (1995).
 - [5] M. Brune, F. Schmidt-Kaler, A. Maali, J. Dreyer, E. Hagley, J. M. Raimond, and S. Haroche, *Phys. Rev. Lett.* **76**, 1800–1803 (1996).
 - [6] H. J. Carmichael, P. Kochan, and B. C. Sanders, *Phys. Rev. Lett.* **77**, 631 (1996).
 - [7] B. C. Sanders, H. J. Carmichael, and B. F. Wielinga, *Phys. Rev. A* **55**, 1358 (1997).
 - [8] L. Horvath, B. C. Sanders, and B. F. Wielinga, *J. Opt. B: Quant. and Semiclassical Opt.* **1**(4), 446 (1999).
 - [9] E. T. Jaynes and F. W. Cummings, *Proc. IEEE* **51**, 89 (1963).
 - [10] M. G. Raizen, R. J. Thompson, R. J. Brecha, H. J. Kimble, and H. J. Carmichael, *Phys. Rev. Lett.* **63**, 240 (1989).
 - [11] Y. Zhu, D. J. Gauthier, S. E. Morin, Q. Wu, H. J. Carmichael, and T. W. Mossberg, *Phys. Rev. Lett.* **64**, 2499 (1990).
 - [12] R. J. Thompson, G. Rempe, and H. J. Kimble, *Phys. Rev. Lett.* **68**, 1132 (1992).